



Phylogenomic analysis of evolutionary relationships in *Ranitomeya* poison frogs (Family Dendrobatidae) using ultraconserved elements

Morgan R. Muell^{a,b,*}, Germán Chávez^{c,d}, Ivan Prates^e, Wilson X. Guillory^{a,f}, Ted R. Kahn^g, Evan M. Twomey^h, Miguel T. Rodriguesⁱ, Jason L. Brown^a

^a School of Biological Sciences, Southern Illinois University, Carbondale, IL 62901, USA

^b Department of Biological Sciences, Auburn University, Auburn, AL, USA

^c Instituto Peruano de Herpetología, Lima, Perú

^d División de Herpetología – CORBIDI, Lima, Perú

^e Department of Ecology and Evolutionary Biology, University of Michigan, Ann Arbor, MI, USA

^f Department of Biological Sciences, Rutgers University Newark, Newark, NJ, USA

^g Species Survival Commission (SSC), International Union for Conservation of Nature (IUCN), Gland, Switzerland

^h Faculty of Biological Sciences, Goethe University, Frankfurt am Main, Germany

ⁱ Instituto de Biociências, Universidade de São Paulo, São Paulo, Brazil

ARTICLE INFO

Keywords:

Ranitomeya

UCEs

Divergence time estimation

Phylogenomics

Dendrobatidae

Amphibians

ABSTRACT

The use of genome-scale data in phylogenetics has enabled recent strides in determining the relationships between taxa that are taxonomically problematic because of extensive morphological variation. Here, we employ a phylogenomic approach to infer evolutionary relationships within *Ranitomeya* (Anura: Dendrobatidae), an Amazonian lineage of poison frogs consisting of 16 species with remarkable diversity in color pattern, range size, and parental care behavior. We infer phylogenies with all described species of *Ranitomeya* from ultraconserved nuclear genomic elements (UCEs) and also estimate divergence times. Our results differ from previous analyses regarding interspecific relationships. Notably, we find that *R. toraro* and *R. defleri* are not sister species but rather distantly related, contrary to previous analyses based on smaller genetic datasets. We recover *R. uakarii* as paraphyletic, designate certain populations formerly assigned to *R. fantastica* from Peru as *R. summersi*, and transfer the French Guianan and eastern Brazilian *R. amazonica* populations to *R. variabilis*. By clarifying both inter- and intraspecific relationships within *Ranitomeya*, our study paves the way for future tests of hypotheses on color pattern evolution and historical biogeography.

1. Introduction

Many aposematic organisms exhibit high intraspecific variation in coloration, likely due to a combination of natural and sexual selection (Noonan and Comeault, 2009). However, some converge on similar warning signals via Müllerian mimicry (Kapan 2001; Sherratt 2008), a phenomenon well-documented in *Heliconius* butterflies (Mallet and Gilbert Jr., 1995). In vertebrates, high aposematic diversity as well as mimicry is found in Neotropical poison frogs (Dendrobatidae) (Noonan and Comeault, 2009; Prates et al., 2019; Summers et al., 2003), which has greatly challenged taxonomists working on this group (Wollenberg et al., 2006), especially in the absence of genetic data. Among dendrobatid genera, *Ranitomeya* has been particularly troublesome (Brown et al., 2011b), but offers perhaps the greatest diversity of color patterns

and mating systems whose study would benefit from better knowledge of its phylogenetic relationships.

Ranitomeya is currently composed of 16 species characterized by small size, pale reticulated limbs, and shorter first than second fingers (Brown et al., 2011b). Some species possess high intraspecific diversity in color pattern while others are monomorphic. Color pattern diversity is decoupled from species range size; there are monomorphic species with both narrow (e.g., *R. yavaricola*) and wide (e.g., *R. toraro*) ranges, and polymorphic species with narrow (e.g., *R. imitator*, *R. fantastica*) and wide (e.g., *R. variabilis*, *R. uakarii*) ranges. Most species occupy forested areas of the upper Amazon drainage in Peru, Ecuador, and Colombia, though others have dispersed into the Amazon basin as far east as French Guiana (Brown et al., 2011b).

Ranitomeya systematics and taxonomy have proven challenging to

* Corresponding author at: Department of Biological Sciences, Auburn University, Auburn, AL 36849, USA.

E-mail address: mrm0161@auburn.edu (M.R. Muell).

<https://doi.org/10.1016/j.ympev.2022.107389>

Received 23 December 2020; Received in revised form 14 November 2021; Accepted 17 November 2021

Available online 10 January 2022

1055-7903/© 2022 Elsevier Inc. All rights reserved.

disentangle. In contrast to their large diversity in color and pattern, they display little anatomical (e.g., osteological) variation, limiting the utility of morphological data in systematic and phylogenetic analyses. These issues are compounded by Müllerian mimicry among sympatric species, which makes them difficult to classify in the absence of call data. For example, *R. imitator* mimics the color and pattern of *R. summersi*, *R. fantastica*, and *R. variabilis* across its range (Symula et al., 2001; Stuckert et al., 2014), and Müllerian mimicry may occur in other species as well (e.g., *R. reticulata* and *R. amazonica*) (Brown et al., 2011b).

Ranitomeya is currently organized into four species groups: the *reticulata* group (six species: *benedicta*, *fantastica*, *reticulata*, *summersi*, *uakarii*, and *ventrimaculata*), the *variabilis* group (two species: *amazonica* and *variabilis*), the *defleri* group (two species: *defleri* and *toraro*), and the *vanzolinii* group (six species: *cyanovittata*, *flavovittata*, *imitator*, *sirensis*, *vanzolinii*, and *yavaricola*) (Brown et al., 2011b). Group organization has previously been determined by monophyly, phenotype, mating system, and call differences (Brown et al., 2008, 2011b; Perez-Peña et al., 2010). Several outstanding questions persist regarding the systematic relationships of each species group in *Ranitomeya*, with studies using different methods and datasets having found conflicting relationships. For example, *R. toraro* was inferred as sister to *R. defleri* by Brown et al. (2011a), forming a clade sister to the *reticulata* group. However, Grant et al. (2017) found that this clade is sister to the *variabilis* group, not the *reticulata* group. Thus, the phylogenetic placement of *R. defleri* and *R. toraro* remains unclear. Furthermore, preliminary analyses of morphology suggest a divide between northern and southern populations of *R. uakarii* from the *reticulata* group in Peru (Brown et al., 2011b, Brown et al., unpub. data). *Ranitomeya uakarii* has three distinct morphs (sensu Brown et al., 2011b): the “nominal” morph from the Loreto region of northern Peru (Brown et al., 2006); the “Toraro” morph, a potential mimic of *R. toraro* located south of the “nominal” populations near Acre, Brazil and the Madre de Dios province of Peru; and the “Tri-country” morph, a genetically unsampled morph from southeastern Colombia near the three-country corner of Peru, Colombia, and Brazil (Brown et al., 2011b). These geographic factors suggest further genetic investigation of intraspecific relationships within *R. uakarii*. Lastly, relationships in the *vanzolinii* group are in flux. Particularly, the phylogenetic placement of *R. cyanovittata* and *R. yavaricola* in relation to other species in the group has varied in studies since those species’ description by Perez-Peña et al., 2010 (Brown et al., 2011b, Grant et al., 2017).

Previous phylogenetic studies of *Ranitomeya* have been hindered by limited genetic and taxon sampling. Almost all previous studies have used mitochondrial data (Summers et al., 1997; Summers et al., 1999; Clough and Summers, 2000; Vences et al., 2000; Symula et al., 2001; Santos et al., 2003; Symula et al., 2003; Darst and Cannatella, 2004; Noonan and Wray, 2006; Roberts et al., 2006), or a combination of mitochondrial data and a handful of nuclear loci (Brown et al., 2008, 2011b; Perez-Peña et al., 2010; Pyron and Wiens, 2011; Santos et al., 2009; Twomey and Brown, 2008), in some cases combined with morphological characters (Grant et al., 2006; Grant et al., 2017). Guillory et al. (2019) used ultraconserved elements to build a phylogeny for Dendrobatidae, but included a limited set of *Ranitomeya* species. Comprehensive sampling of genomic markers in all *Ranitomeya* species, with additional sampling from representative populations of widespread or variable species, would greatly improve our knowledge of species limits in these frogs.

In this study, we provide a new phylogeny for *Ranitomeya* based on comprehensive sampling of genetic markers, species, and morphotypes spanning the distribution of the genus in northern South America. We estimate divergence times and delimit species boundaries and use this information to propose paleogeographic scenarios that may have shaped the present biogeography of *Ranitomeya*. We also propose a revised taxonomy for *Ranitomeya*, with the goal of providing clarity for future studies of dendrobatid color and reproductive evolution.

2. Materials and methods

2.1. Data collection

We collected DNA samples from 65 *Ranitomeya* individuals from all 16 currently described *Ranitomeya* species (Table S1). These individuals broadly represent the known genetic, geographic, and phenotypic diversity exhibited across the genus. *Andinobates minutus* and *Excidobates captivus* served as outgroup taxa, for a total of 67 samples. We extracted DNA of toe or liver tissue using the Qiagen DNeasy Blood and Tissue Kit (Valencia, California), and sent extracted DNA to RAPiD Genomics (Gainesville, Florida), where library preparation and Illumina sequencing of ultraconserved elements (UCEs) were performed following standard protocols (Faircloth et al., 2012). We used the Tetrapods-UCE-5Kv1 probe set to enrich the samples, targeting 5060 UCE loci with 5472 probes. We used ultraconserved elements (UCEs) because of their high utility at both shallow and deep evolutionary timescales (Faircloth et al., 2012). UCEs consist of a highly conserved core region with flanking sequences of increasing variability as distance from the core increases, and have been used successfully in previous phylogenomic studies of dendrobatids (Guillory et al., 2019; Guillory et al., 2020).

2.2. Bioinformatics

We trimmed the raw reads with Illumiprocessor v2.0.6 (Faircloth, 2013) through the software PHYLUCe v1.5.0 (Faircloth, 2016), a standard pipeline for processing UCE datasets. Illumiprocessor is a Python-based wrapper for Trimmomatic v0.36 (Bolger et al., 2014). We used Trinity v1.6 (Grabherr et al., 2011) to assemble most of our samples and Velvet v1.2.10 (Zerbino and Birney, 2008) to assemble one sample (ID: 0915), all with default parameters. We mapped these assembled contigs to UCE loci with PHYLUCe and aligned each locus with MUSCLE v3.8.31 (Edgar, 2004). We initially filtered captured loci for 70% matrix completeness, and then further filtered for the top 75% most informative loci based on parsimony-informative sites with a custom R v3.2.3 script (R Core Team, 2015) implementing the PHYLOCH v1.5–5 package (Heibl, 2008). Both these steps helped to prevent inaccurate results in our coalescent-based analysis due to a bias toward the influence of less informative loci (Hosner et al., 2016). We used the resulting dataset for all further analyses.

2.3. Phylogenetic analyses

We used two phylogenetic approaches to analyze our data. To infer relationships among all samples and identify putative species within our dataset, we first inferred a maximum likelihood tree from a concatenated matrix with IQ-TREE v1.5.5 (Nguyen et al., 2015). We ran IQ-TREE with 10,000 ultrafast bootstrap replicates (Minh et al., 2013), the GTR substitution model, empirical base frequencies, and a free-rate model of rate heterogeneity with four categories. We used ModelFinder to determine these best-fitting parameters (Kalyaanamoorthy et al., 2017) with AICc as an optimality criterion. Because UCEs do not necessarily encode proteins, there is no evidence to support any particular partitioning scheme for them (Streicher and Wiens, 2017). However, we ran a second analysis partitioning our matrix by locus, using ModelFinder to determine a substitution model for each locus, to see whether partitioning by locus produced a better tree. We did not use PartitionFinder to identify the best partitioning scheme due to analytical time constraints.

To assess topological variation, we also calculated gene concordance factors (gCF) and site concordance factors (sCF) for our unpartitioned and partitioned trees to measure the proportion of gene trees and sites respectively that contain each branch (Minh et al., 2020). Prior to this analysis, we used IQ-TREE to generate gene trees for each UCE locus in our filtered dataset. For each gene tree, we used ModelFinder to select a

nucleotide substitution model and IQ-TREE's -czb option (collapse zero branch lengths) to reduce branches with lengths near zero to polytomies, reducing gene tree bias in later analyses (Persons et al., 2016).

As a complement to IQ-TREE, we also used the coalescent method ASTRAL-III v5.6.1 (Zhang et al., 2018) to generate a species tree that accounts for incomplete lineage sorting. As opposed to IQ-TREE, ASTRAL-III can detect discordant topological signals in aggregated gene trees and present a species tree topology accounting for them. All 16 *Ranitomeya* species sensu Brown et al. (2011b), plus two outgroups and three additional terminals representing *R. aff. uakarii* and *biolat* populations of *R. sirensis* (see results), were specified as putative species in the requisite mapping file provided to ASTRAL, predicated on the prior IQ-TREE results. These putative species assignments were predicated on IQ-TREE results, meaning that any individual samples we found grouped with different species than taxonomy sensu Brown et al. (2011b) were assigned to their new species grouping rather than their grouping under the old taxonomy. We used the same gene trees calculated for generating gCF and sCFs as inputs for our ASTRAL analysis.

To test for statistical support for incongruent phylogenetic topologies, we used the Swofford–Olsen–Waddell–Hillis (SOWH) test (Swofford et al. 1996). It is commonly applied to determine if the maximum likelihood tree in a phylogenetic analysis is significantly different from an alternative hypothesis (Goldman et al. 2000). The SOWH test compares the observed difference in log-likelihood between two topologies to a null distribution of differences in log-likelihood generated by parametric resampling (Church et al. 2015). We ran SOWH topology tests in SOWHAT (<https://github.com/josephryan/SOWHAT>; Church et al. 2015) for 100 generations per alternative hypothesis using RAXML

and a GTR substitution model with a free-rate model of rate heterogeneity with four categories. The best unconstrained maximum likelihood tree perfectly matched the IQ-TREE topology (Fig. 1).

2.4. Divergence time estimation

To understand the timing of diversification in *Ranitomeya*, we estimated divergence times with MCMCTree in PAML v4.8 (Yang, 2007). Divergence time estimation from large genomic datasets can be computationally challenging, but MCMCTree allowed us to use all UCE loci in a feasible amount of time. We used our IQ-TREE topology as a reference topology as it included all samples. We chose our maximum likelihood topology because a dated tree based only on species-level relationships would not fully explore and take advantage of our taxon sampling, one of the major strengths of this dataset. We used an independent rates clock model for rate priors because we expect our broad interspecific sampling will lead to branch-specific, heterogeneous rates of evolution, violating the rate homogeneity assumptions of a strict molecular clock.

Tree calibration was challenged by the lack of a fossil record for dendrobatid frogs. Santos et al. (2009) dated the origin of Dendrobatidae by time-calibrating a pan-Amphibia tree with paleogeographic and fossil data, and used this estimate to in turn time-calibrate a Dendrobatidae tree under three different paleogeographic scenarios. We averaged the means and standard deviations of divergence times for the node corresponding to the divergence of *Ranitomeya* and *Andinobates* across each of the three scenarios, calculating a mean divergence time of 12.651 Ma and a standard deviation of 2.576 Ma. We then used these

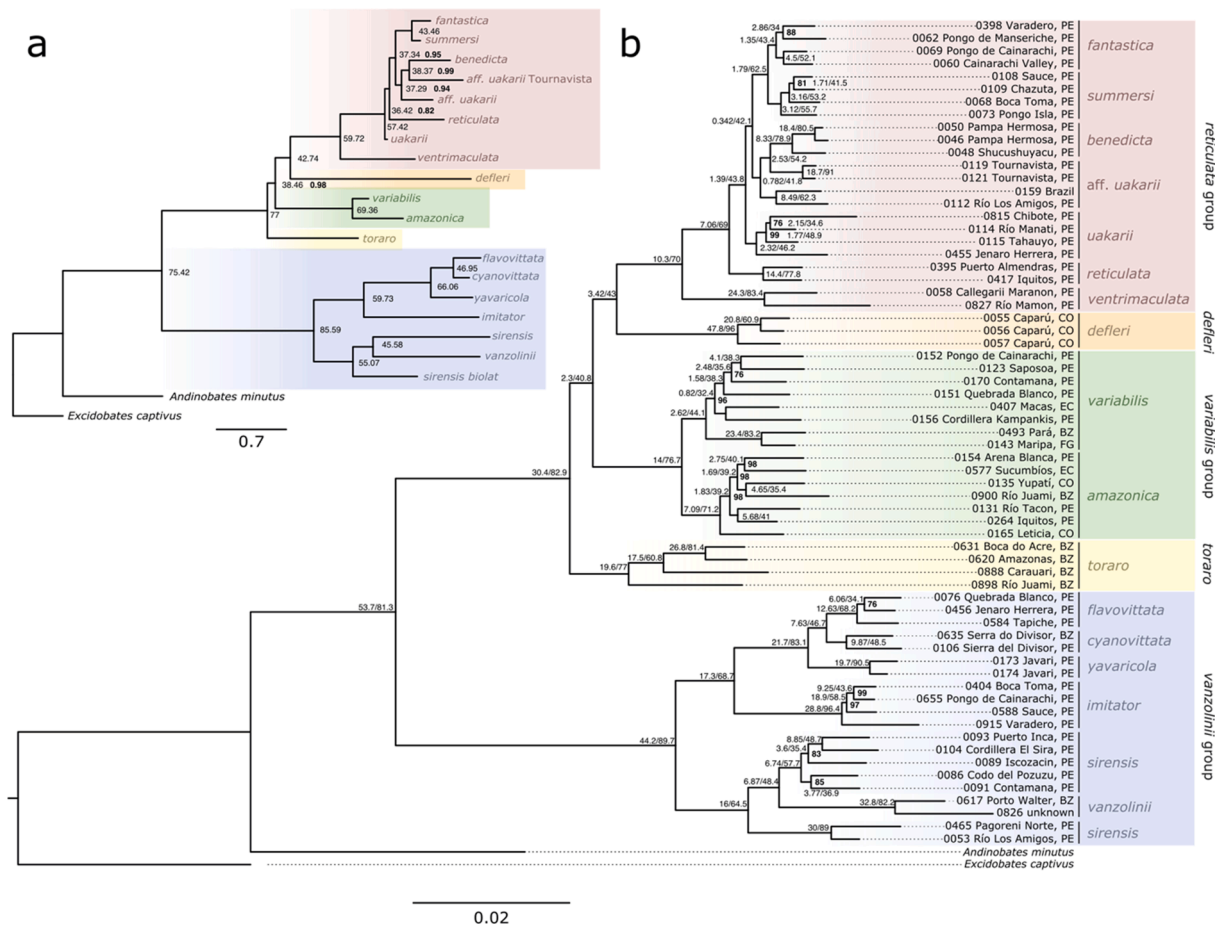


Fig. 1. a. Species tree generated by ASTRAL. Values to the right of nodes are quartet scores (range 0 to 100), and bolded support values to the right of quartet scores are posterior probabilities below 1 (range 0 to 1). b. Maximum likelihood tree generated in IQ-TREE from the unpartitioned matrix. Bootstrap values under 100 are bolded and are shown to the right of nodes. Values separated by a slash are the gCF and sCF values, respectively, for that branch.

values to set a uniform distribution on the calibration node corresponding to the divergence between *Ranitomeya* and *Andinobates* between 7.601 and 17.701 Ma, constructing a 95% confidence interval around the mean 12.651 Ma. We first ran the MCMCTree analysis without sequence data to assess whether our model parameters produced reasonable priors from our calibration. To expedite the analysis, we then used BASEML (also in PAML) to calculate approximate branch length values prior to running MCMCTree, under an HKY substitution model. We used the HKY model due to computational constraints encountered when we tried to run the GTR model, which more closely matched the model chosen by our ModelFinder results in IQ-TREE. The GTR model was likely too parameter-rich for our computational resources, so we chose the HKY model because it was next closest in complexity. We ran MCMCTree for 2,000,000 burn-in generations and subsequently sampled every 1,000 generations until we obtained 20,000 samples across a total of 22,000,000 iterations. To assess convergence, we ensured ESS values for each node were over 200 using Tracer v1.7.1 (Rambaut et al., 2018), and ran our analysis twice from two different random starting seeds before confirming that both converged to similar posterior estimates.

3. Results and discussion

3.1. UCE sequence capture

We captured 2664 loci in our initial dataset. After filtering for 70% matrix completeness, our dataset consisted of 1568 loci. After we filtered further for the top 75% most informative loci by parsimony-informative sites, we retained 1176 loci with 72,828 parsimony-informative sites in our final dataset.

3.2. Phylogenetic analyses

Our maximum likelihood phylogenies, both unpartitioned (Fig. 1b) and fully partitioned (Fig. S1), were very similar with high bootstrap support values and highly similar distributions of gCF and sCF values (Figure S2). In both unpartitioned and fully partitioned trees, 90% of bootstrap values were above 90 (Fig. 1b; Figure S1), however gCF and sCF values were generally low with mean values of 11.74 and 58.67 respectively (Figure S2). These low gCF and sCF values are indicative of gene tree discordance, similar to that occurring in *Ameerega* poison frogs (Guillory et al., 2020). These conflicts may be resolved by more fine-scale intraspecific sampling in future studies. Our ASTRAL analysis yielded an almost identical topology to the unpartitioned maximum likelihood tree, with the exception that *R. reticulata* switched places with the northern *R. uakarii* individuals (*uakarii*, Fig. 1a). Quartet scores for intraspecific differences, such as reassignment of some populations to different species, tended to be lower, likely due to the difficulty of resolving shorter, more recent branches. Regardless, all intraspecific differences discussed here were recovered in both the unpartitioned and fully partitioned maximum likelihood trees (Fig. 1b; Fig. S1).

Our analyses generally recovered long-recognized species groups as clades within *Ranitomeya*; this is the case for the *reticulata*, *variabilis*, and *vanzolinii* groups. However, in our unpartitioned analysis we found that *R. toraro* and *R. defleri* were not closely related, contradicting previous findings that they form a monophyletic *defleri* group (Brown et al. 2011b; Grant et al., 2017). Instead, we found that *R. defleri* is sister to the *reticulata* clade, while *R. toraro* is sister to the common ancestor of *R. defleri* and the *reticulata* clade (SOWH tests, P-value < 0.01, Table 1: H1). Our fully partitioned analysis recovered *R. toraro* as sister to *R. defleri* and the *reticulata* clade. However, this node only had a bootstrap support value of 81, indicating lower sampling variance and lower support than the node recovered by the unpartitioned analysis (Fig. S1). Additionally, gCF and sCF values at this node in the unpartitioned tree, 30.4 and 82.9 respectively, were higher than the values at the partitioned tree, values 2.9 and 34.3 respectively (Fig. 1b; Fig. S1). Our

Table 1

Results of SOWH topology tests. All lower CIs were < 0.01 and all upper CIs are equal to 0.036. Alternative topologies reflect results of Brown et al. (2011b) and are summarized in Fig. S3.

Hypothesis*	ML of best unconstrained tree	ML of best constrained tree	Δ lnL	P-value
H1: <i>R. defleri</i> and <i>R. toraro</i> as reciprocally monophyletic sister taxa	-1578853.57	-1579097.46	243.89	<0.01
H2: Monophyly of Eastern <i>R. variabilis</i> and <i>R. amazonica</i>	-1578853.61	-1579026.92	173.31	<0.01
H3: Monophyly of <i>R. fantastica</i> , <i>R. summersi</i> Boca Toma, and <i>R. summersi</i> Ponga Isla	-1578853.61	-1579551.32	697.71	<0.001
H4: Monophyly of all <i>R. uakarii</i> (including <i>R. aff. uakarii</i>)	-1578853.58	-1579723.80	870.22	<0.001
H5: Monophyly of <i>R. aff uakarii</i>	-1578853.61	-1579128.09	274.48	<0.001
H6: Monophyly of <i>R. sirensis</i>	-1578853.59	-1579267.41	413.82	<0.001

ASTRAL analysis supports the unpartitioned topological placement of *R. toraro* with a high quartet score of 77.

We also found that our eastern *R. amazonica* samples from Maripa in French Guiana (0143) and Pará in Brazil (0493) are nested within *R. variabilis* (SOWH test, P-value < 0.01, Table 1: H2). Further, our analysis inferred that *R. uakarii* is split into two major groups: one, occupying the southern range of the species, is more closely related to *R. benedicta* (*aff. uakarii*, in Fig. 1b); the remaining sampled *R. uakarii* populations form a clade sister to another clade consisting of *R. fantastica*, *R. summersi* and those southern *R. uakarii* populations (*uakarii*, Fig. 1b), rendering *R. uakarii* paraphyletic (SOWH tests, P-value < 0.01, Table 1: H2–H4). Lastly, within the *vanzolinii* group, we found that *R. sirensis* is not monophyletic. Instead, two *R. sirensis* samples from southern Peru corresponding to the formerly recognized *R. biolat* sensu Morales (1992) were sister to a clade containing the remaining *R. sirensis* samples and *R. vanzolinii* (Fig. 1b; SOWH tests, P-value < 0.01, Table 1: H6). With the exception of the placements of *R. defleri* and *R. toraro*, all of these findings were present in both the partitioned and unpartitioned trees.

3.3. Revised species groups in *Ranitomeya*

Ranitomeya toraro species group. One species: *R. toraro* (Brown et al., 2011a).

Ranitomeya defleri species group. One species: *R. defleri* (Twomey and Brown, 2009).

Ranitomeya reticulata species group. A monophyletic assemblage of six species: *Ranitomeya reticulata* (Boulenger, 1884 “1883”); *R. fantastica* (Boulenger, 1884 “1883”); *R. ventrimaculata* (Shreve, 1935); *R. uakarii* (Brown et al., 2006); *R. summersi* (Brown et al., 2008) and *R. benedicta* (Brown et al., 2008).

Ranitomeya variabilis species group. A monophyletic assemblage of two species: *Ranitomeya variabilis* (Zimmermann and Zimmermann, 1988) and *Ranitomeya amazonica* (Schulte, 1999).

Ranitomeya vanzolinii species group. A monophyletic assemblage of six species: *Ranitomeya vanzolinii* (Myers, 1982); *R. sirensis* (Aichinger, 1991); *R. imitator* (Schulte, 1986); *R. flavovittata* (Schulte, 1999); *R. yavaricola* (Perez-Peña et al., 2010) and *R. cyanovittata* (Perez-Peña

et al., 2010).

3.4. Systematic implications

3.4.1. The *reticulata* group

The *reticulata* group is a monophyletic group of six described species. All species possess vocalizations consisting of a series of short buzz-like notes (0.1–0.5 s in length) given in rapid succession (100–200 notes per minute; Brown et al., 2011b). Most members of this group possess red or orange pigmentation concentrated on the head. In general, most of the relationships we resolved within this group are consistent with previous phylogenetic and taxonomic studies (Brown et al., 2011b). However, there are noteworthy differences from previous studies regarding the relationships between samples assigned to *R. fantastica* and *R. uakarii*. First, we consistently recover *R. uakarii* as paraphyletic (Fig. 1; Fig. S1), with the “nominal” morph (sensu Brown et al., 2011b; hereafter considered *R. uakarii*; Fig. S4G–I) forming a clade sister to a clade containing *R. fantastica*, *R. benedicta*, *R. summersi*, and the *R. uakarii* “Toraro” morph (sensu Brown et al., 2011b; hereafter considered *R. aff. uakarii*; Fig. S4J and K). *Ranitomeya aff. uakarii* is sister to *R. benedicta* (Fig. 1; Figs. S3I and S4W–X). These results differ from previous studies with intraspecific sampling of *R. uakarii* which recovered the species as monophyletic (Brown et al., 2006; Brown et al., 2011b), and suggest that *R. aff. uakarii* may merit specific status, which is supported by their unique coloration pattern.

The elevation of *R. aff. uakarii* to species status would rectify the paraphyly of *R. uakarii* sensu stricto; however, paraphyly in *R. aff. uakarii* would not be entirely reconciled because of the sister relationship between *R. benedicta* and the Tournavista populations of *R. aff. uakarii*. We suspect that the Tournavista populations of *R. aff. uakarii* (sample IDs 0119 and 0121), which are sister to *R. benedicta* yet most similar in pattern to *R. uakarii* (Fig. S4 & Fig. S5), may reflect historical introgression between the ancestor to *R. benedicta* and *R. aff. uakarii*. For the time being, we recommend additional investigation into morphological and population-level genetic differences between *R. uakarii* and *R. aff. uakarii* to decide whether the “Toraro” morph deserves specific status. We could not assess where the “Tri-country” morph was placed in the phylogeny due to a lack of sequenced samples; however, we suspect that because their range occurs north of the “nominal” *R. uakarii* individuals in this analysis, they are more likely to be more closely related to *R. uakarii* than *R. aff. uakarii*.

Our phylogenomic results also necessitate a redefinition of *R. summersi* (Brown et al., 2008). Our results match those of Brown et al. (2011b), where individuals previously assigned to *R. fantastica* from the lower Huallaga River populations at Boca Toma and Pongo Isla in Peru (sample IDs 0068 and 0073 respectively) are actually nested within *R. summersi*. As discussed by Brown et al. (2011b), it appears these individuals were erroneously ascribed to *R. fantastica*. Based on their similar morphology to *R. summersi* – that is, black coloration with bright-orange dorsal and limb striping (Fig. S4D) – and our phylogenomic results, we consider these populations members of *R. summersi*. On the other hand, it is currently unclear whether misidentification might also explain the unexpected placement of these former *R. fantastica* populations (Fig. S4C) as members of the *R. summersi* clade. Historical introgression may have occurred between *R. fantastica* and *R. summersi* at the Boca Toma and Pongo Isla sites. Resolution of this issue will likely require increased population-level sampling in this region.

We acknowledge the possibility that *R. fantastica* and *R. summersi* may constitute a single species. Outside the single population of *R. fantastica* near Tarapoto (close to *R. summersi* Boca Toma and Pongo Isla sites), all other known populations of *R. fantastica* and *R. summersi* segregate on the basis of both dorsal color pattern and genetics, supporting the conclusion that *R. summersi* and *R. fantastica* are distinct species. In addition, Twomey et al. (2020) found that *R. summersi* contains distinct skin pigments from *R. fantastica*. Specifically, *R. summersi* contained a suite of red carotenoids that are likely metabolic derivatives

of dietary carotenoids, whereas *R. fantastica* lacked red carotenoids. This difference represents a clear character diagnosing the two taxa, albeit a difficult character to assess without skin pigment analyses. Overall, the available data tend to support the continued recognition of these two taxa.

3.4.2. The *variabilis* group

The *variabilis* group contains two species: *R. variabilis* (Zimmermann and Zimmermann, 1988) and *R. amazonica* (Schulte, 1999). The two species both exhibit a promiscuous mating strategy with male parental care, and have regularly spaced, buzzing vocalizations 0.16–0.44 s in length at a rate of 24–70 notes per minute (Brown et al., 2011b). Most of our phylogenomic results are consistent with previously recovered relationships (Brown et al., 2011b), except that we find samples from French Guiana (sensu Brown et al., 2011b; sample ID 0143, Fig. S5N–P) and the Pará region of Brazil (sample ID 0493), originally assigned to *R. amazonica*, to be nested within *R. variabilis*. These eastern populations are similar morphologically to striped *R. variabilis* populations found at many sites in the Loreto and San Martín provinces of Peru, including yellow dorsolateral stripes and a lack of reddish pigmentation, although it is unclear if this coloration is conserved or evolved independently. Based on these updated results, we tentatively consider them members of *R. variabilis* (see Fig. S6 for a detailed map clarifying distributions for these taxonomic changes). Our two eastern *R. variabilis* samples were sister to each other (Fig. 1) and diverged from the common ancestor of the other *R. variabilis* populations around 3.3 Ma (see section 3.5 below). This branch is relatively long compared to time between divergence events of other *R. variabilis* samples (Fig. 2), indicating they have been geographically isolated for longer than other *Ranitomeya* populations sampled in this dataset. Future studies should include more genetic samples of *R. variabilis* populations not represented in this study, such as those found in other parts of Pará.

3.4.3. The *vanzolinii* group

Phylogenetic relationships of species in the *vanzolinii* group are uncertain, and resolving them requires both more extensive sampling and interrogative analyses into potential patterns of hybrid introgression and population genetic structure. In this study, we found strong support for paraphyly in *R. sirensis*, largely with respect to previously recognized species boundaries of *R. lamasi* and *R. biolat* sensu Morales (1992), which were synonymized with *R. sirensis* by Brown et al. (2011b) based on genetics, behavior and morphology. We recovered one group of *sirensis* samples sister to *vanzolinii* and another group of samples sister to the clade containing both *vanzolinii* and *sirensis* samples. The former group includes *R. sirensis* sensu stricto as well as *R. lamasi* sensu Morales (1992), while the latter group includes samples from southern Peru and corresponds, at least geographically, to *R. biolat* sensu Morales (1992). In particular, the long branch separating the *R. biolat* samples and its sister clade containing *R. vanzolinii* and the other *R. sirensis* samples, dated between 3 and 7 Ma (see section 3.5 below), suggests that *R. biolat* could be a legitimate species. The restoration of *R. biolat* to specific status would render *R. sirensis* monophyletic.

Other interspecific relationships in the *vanzolinii* group were surprising, especially the recovery of *R. vanzolinii* as closely related to *R. sirensis*. *Ranitomeya vanzolinii* has almost always been recovered as sister to *R. flavovittata* in previous studies that included both species (Brown et al., 2011b; Grant et al., 2017; Perez-Peña et al., 2010; Roberts et al., 2006; Twomey and Brown, 2008), whereas *R. sirensis* has been inferred as sister to the remaining species in the *vanzolinii* group. While our results were derived from nuclear genomic data, many previous studies in the *vanzolinii* group have relied on mitochondrial data (Noonan and Wray, 2006; Perez-Peña et al., 2010; Roberts et al., 2006; Symula et al., 2003; Twomey and Brown, 2008), which could partially explain why our results contradict previous analyses. Overall, more detailed genomic studies will be required to verify these unexpected results.

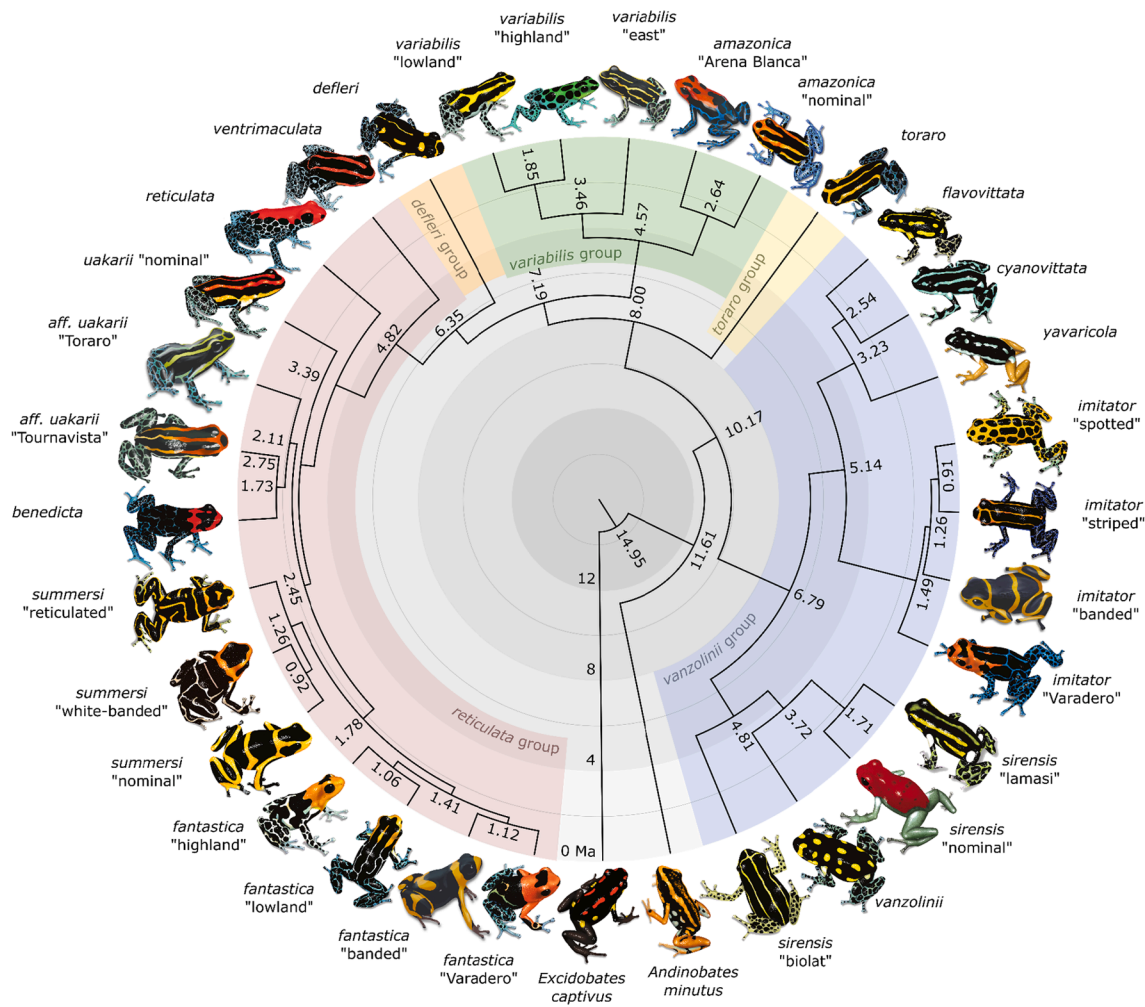


Fig. 2. Time-calibrated phylogeny for *Ranitomeya* and two outgroups generated using MCMCTree. Each terminal represents a morph within a species. Time units are millions of years. Species groups are highlighted and labeled. Frog illustrations by TRK and WXG. For detailed MCMCTree results see Fig. S7 and Table S2.

3.5. Divergence time estimation

Our two MCMCTree runs converged, with ESS values well above 200 and nearly identical mean divergence times at each node (Table S2; Fig. S7). Our estimates show that the common ancestor of *Ranitomeya* diverged from its sister genus *Andinobates* approximately in the middle Miocene 11–12 Ma, which is unsurprisingly similar to the date of this node recovered by Santos et al. (2009) that we used to calibrate this analysis. Overall, the rest of our divergence times were slightly younger than those recovered by Santos et al. (2009), despite using a dated node from their study as our time-calibration—likely a result of using different genetic markers (UCEs vs. two mitochondrial loci and one nuclear locus). Diversification in the group was initially relatively slow until an apparent increase about 4–6 Ma, especially in the *reticulata* clade. Our divergence time estimates were very similar to those found by Guillory et al. (2019) in their analysis of the Dendrobatidae phylogeny, likely because they also used UCEs and calibrated their tree using estimates derived by Santos et al. (2009). Notably, Guillory et al. (2019) used BEAST based on the top 200 most informative loci in their divergence time estimation, compared with our use of our entire dataset in MCMCTree.

3.6. Biogeographic implications

Our phylogenetic results also provide insights into the biogeographic history of *Ranitomeya*. The nexus of *Ranitomeya* diversity is east-central

and northeastern Peru, with comparatively little species diversity in the greater Amazon basin (Fig. 3; Fig. S7), similarly to the dendrobatid genus *Ameerega* (Guillory et al., 2020). A principal question is whether the recent and dynamic paleogeographic history of Amazonia contributed to the diversification of *Ranitomeya*, most notably the orogeny of the Andean cordillera. The recent uplift of the Andes in the Late Miocene has long been a suggested principal driver of Neotropical diversification (Hoorn et al., 2010). The orogeny and resulting topographic heterogeneity in the region likely fomented the diversification of *Ranitomeya* and other dendrobatids by generating new local-scale climatic regimes, ecological niches, and geographic barriers to gene flow. The divergence between *Ranitomeya* and its sister genus *Andinobates* at around 12 Ma (Fig. 2) corresponds to an intense period of uplift in the central Andes (Hoorn et al., 2010).

A few studies have debated whether Andean dendrobatids originated in the Amazonian highlands (the foothills of the Andes), or in the Amazonian lowlands to the east (Roberts et al., 2006; Brown and Twomey, 2009). Brown and Twomey (2009) and Guillory et al. (2020) both suggested an Andean origin for the poison frog genus *Ameerega*, and here we propose a similar history for *Ranitomeya*. This was also inferred by Santos et al. (2009), who used ancestral range estimation to show that *Ranitomeya* dispersed from the Andes into the Amazon basin beginning around 10 Ma. A marine incursion in northern South America during the Miocene, which created the Pebas “megawetland” system east of the rising Andes (Hoorn et al., 2010), likely limited *Ranitomeya* to the Andes. When the megawetland receded around 10 Ma, certain

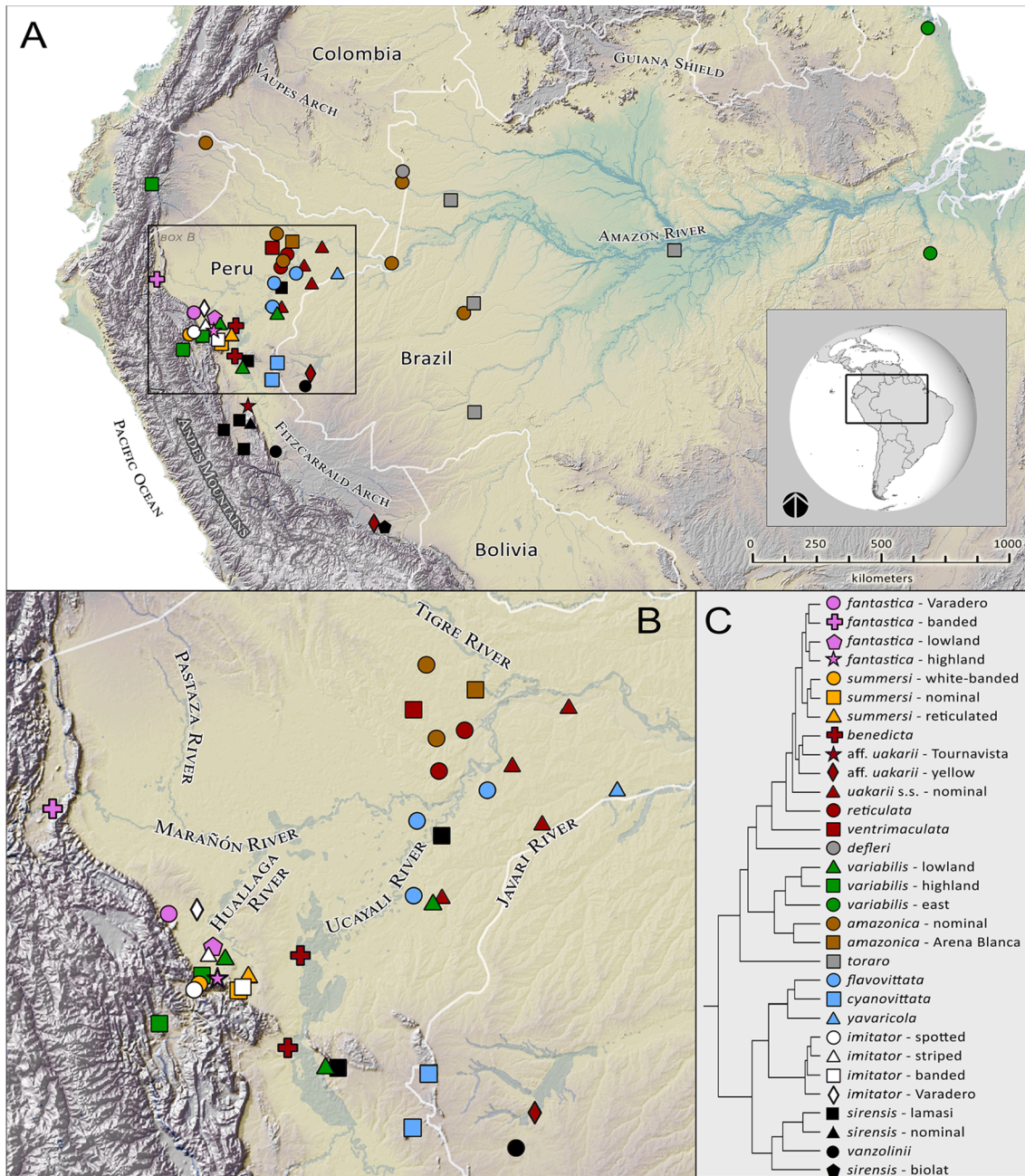


Fig. 3. Map of sequenced *Ranitomeya* localities used in the full 67-terminal phylogeny generated by IQ-TREE. A) The total distribution of *Ranitomeya* throughout South America B) and a closer look at the East Andean Versant. C) The reduced phylogeny on the right contains one tip per morph. Symbols on tips correspond to morph localities on the map. Each species has a common color for all morphs, and different-shaped symbols represent different morphs within that color species. See Fig. S8 for a generalized extent of occurrences for all species.

Ranitomeya lineages likely dispersed into the Amazon Basin; this corresponds to rapid cladogenesis in lowland *Ranitomeya* around this time as discerned by Santos et al. (2009).

Further lines of evidence for the Andean origin of *Ranitomeya* include its closest related genera (*Andinobates* and *Excidobates*) also inhabiting the Andes, and the much higher number of *Ranitomeya* species associated with mid-elevations along the eastern versant of the Andes or in the immediately adjacent Amazonian lowlands, rather than ranging throughout the Amazon Basin to the east. These restricted ranges are also significant for the labile color pattern evolution apparent in *Ranitomeya*, because many species near the Peruvian Andes exhibit Müllerian mimicry with congeners (e.g., *R. fantastica* and *R. imitator* at Varadero, Peru; Symula et al., 2001; Stuckert et al., 2014), and model

species must colonize areas prior to mimic species in order for Müllerian mimicry can evolve. Our divergence time estimates do indicate that the variable morphs of *R. imitator* diverged more recently than their sympatric model species *R. variabilis* and *R. fantastica* (Fig. 2). Additional studies of the history of dispersal in these species should focus on testing this prediction, potentially by incorporating spatial genetic simulations (Brown et al., 2016; Prates et al., 2016).

Remarkably, we inferred populations from French Guiana and eastern Brazil, originally assigned to *R. amazonica*, to be members of *R. variabilis*. This is unexpected because the other populations of *R. variabilis* occur in the Andes of central Peru, some 4500 km to the west. Some geological studies (Rossetti et al., 2005; Campbell Jr. et al., 2006) suggest that the lacustrine conditions of western Amazonia did

not recede until the Pliocene, around 3–6 Ma, allowing a continuous watershed between the Solimões and Amazon Basins to form, followed by consistent rainforest habitat stretching from the Andes to the Atlantic. This potentially facilitated the migration of *R. variabilis* from west to east; these two lineages diverged in the Pliocene around 3–4 Ma (Fig. 2), well within this timeframe. This hypothesis has already been raised to potentially explain the distribution of *Psophia* trumpeters (Ribas et al., 2012). However, it conflicts with the aforementioned explanation for the overall expansion of *Ranitomeya*, which necessitates the Miocene lake system receding several million years earlier (Hoorn et al., 2010).

An alternative hypothesis proposes that the frogs might have dispersed via the Amazon River on vegetation rafts, ultimately establishing populations known as waif populations (Zimmermann and Zimmermann, 1988). These rafts can be frequently observed during the rainy season floating downstream; we have personally observed substantive vegetation rafts with multiple trees, and at times, large masses of soil. This mode of dispersal could also cover thousands of river-kilometers relatively quickly, even in a matter of months (Kozel, 2002). Landslides are common in montane regions, suggesting that vegetation rafts could form with high frequency along rivers in the Andean foothills. These rafts might more easily make landfall in those stretches where the Amazon assumes the form of a highly reticulated river delta, as seen in extreme eastern Brazil and nearby French Guiana, where populations of *R. variabilis* now occur.

These alternative historical scenarios would generate markedly different biogeographic signatures. For instance, a slow terrestrial dispersal would lead to genetic structure fitting an isolation-by-distance pattern throughout the Andes and the Guiana Shield. Conversely, a pattern of mixed, poorly structured genetic diversity among the two regions fitting the riverine-raft mode of dispersal, particularly if down-river populations possess higher proportions of unique polymorphic sites, would be indicative of founder events. While there is currently no evidence supporting undescribed species diversity in wide-ranging taxa such as *R. variabilis*, more intensive spatial sampling could reveal undiscovered populations. Further field surveys and investigations of genetic structure among populations of wide-ranging species such as *R. variabilis* are required to clarify the biogeographic events behind current distribution patterns in *Ranitomeya*.

4. Concluding remarks

We addressed outstanding issues in the phylogenetic systematics of *Ranitomeya* poison frogs based on genome-scale data and comprehensive taxonomic, geographic, and phenotypic sampling. Our results indicate that *Ranitomeya* began diverging rapidly around 4–6 Ma into several clades with diverse color patterns. Contrary to studies based on smaller datasets, we find that *R. toraro* and *R. defleri* are not sister species, but rather two separate species groups, with *R. defleri* sister to the *reticulata* group and *R. toraro* sister to the clade composed of the *reticulata* group and *R. defleri*. Samples formerly assigned to *R. amazonica* from French Guiana and northeastern Brazil were recovered as sister to *R. variabilis*, and we reassign those populations to *R. variabilis*. Lastly, *R. uakarii* is split into two clades nested within the *reticulata* group, one representing samples from the northern *R. uakarii* range and the other consisting of samples from the southern *R. uakarii* range. Our results, specifically our placement of eastern '*R. amazonica*' populations sister to *R. variabilis*, indicate that *Ranitomeya* biogeographic history may be more complicated than previously thought. We suggest additional investigation into population genetic structure to resolve whether the eastward radiation of *Ranitomeya* is the result of gradual dispersal through the Amazonian lowlands followed by extinction in intervening regions, or more rapid dispersal eastward on riverine rafts. Our study demonstrates the ability of genome-scale data to provide new insights into the evolutionary history and species limits even in relatively well-studied groups of organisms. We recommend that future studies seek to expand our

geographic and genomic sampling to address standing questions on color pattern evolution and biogeography in *Ranitomeya* and other poison frog clades.

CRedit authorship contribution statement

Morgan R. Muell: Methodology, Formal analysis, Data curation, Writing – original draft, Visualization. **Germán Chávez:** Investigation, Writing – review & editing. **Ivan Prates:** Investigation, Writing – review & editing. **Wilson X. Guillory:** Methodology, Formal analysis, Data curation, Writing – review & editing, Visualization. **Ted R. Kahn:** Investigation. **Evan M. Twomey:** Investigation, Writing – review & editing. **Miguel T. Rodrigues:** Investigation. **Jason L. Brown:** Conceptualization, Validation, Investigation, Resources, Data curation, Writing – original draft, Writing – review & editing, Visualization, Supervision, Project administration, Funding acquisition.

Declaration of Competing Interest

The authors declare that they have no known competing financial interests or personal relationships that could have appeared to influence the work reported in this paper.

Acknowledgements

We thank Janalee Caldwell (Sam Noble Oklahoma Museum of Natural History), and Frederick Sheldon (Louisiana State University Museum of Natural Science) for providing tissue samples under their care. We thank César Aguilar (MUSM) and Kyle Summers (ECU) for allowing access to specimens and tissues under their care. We are grateful to Andrew J. Mason for advice on divergence time estimation analyses, as well as Jamie R. Oaks and Perry L. Wood Jr. for additional advice regarding analyses. We thank two anonymous reviewers for their feedback, which greatly improved the quality of this manuscript. Paulo Melo-Sampaio, Pedro Peloso, and members of the Rodrigues Lab assisted during fieldwork. Permits were issued by: Brazil's Instituto Chico Mendes de Conservação da Biodiversidade (SISBIO 30309, 36753, 7147) the Servicio Nacional Forestal y de Fauna Silvestre in Peru (R.D.G. 120-2012-AG-DGFFS-DGEFFS, R.D.G. 029-2016-SERFOR-DGGSPPFFS, R.D.G. 405-2016-SERFOR-DGGSPPFFS, R.D.G. 116-2017-SERFOR-DGGSPPFFS, N° 002765-AG-INRENA, N° 061-2003-INRENA-IFFS-DCB, N° 050-2006-INRENA-IFFS-DCB, N° 067-2007-INRENA-IFFS-DCB, N° 083-2017-SERFOR/DGGSPPFFS, N°004-2013-SERNANP-JRCA, and N°016-2010-SERNANP-DGANP), Contrato de Acceso Marco a Recursos Genéticos in Peru (359-2013-MINAGRI-DGFFS-DGEFFS, Ministerio de Agricultura de Peru (Permit Number Code 25397, N° 2904-2012-AGDGFFS-DGEFFS) and the administration of Manu National Park (06-2013-SERNANP-PNM-JEF).

Funding

Much of this research was supported by startup to JLB provided by Southern Illinois University at Carbondale. MRM and WXG are thankful for funding from the Students United in Exploring, Preserving, and Researching Biodiversity (SUPERB) fellowship, funded by the National Science Foundation (NSF), USA (DUE-1564969).

Appendix A. .

Scripts associated with the methods can be found at <https://github.com/morganmuell/RanitomeyaPhylogenomics>.

Appendix B. Supplementary material

Supplementary data to this article can be found online at <https://doi.org/10.1016/j.ymp.2022.107389>.

References

- Aichinger, M., 1991. A new species of poison-dart frog (Anura: Dendrobatidae) from the Serranía de Sira, Peru. *Herpetologica* 47, 1–5.
- Bolger, A.M., Lohse, M., Usadel, B., 2014. Trimmomatic: a flexible trimmer for Illumina sequence data. *Bioinformatics* 30, 2114–2120. <https://doi.org/10.1093/bioinformatics/btu170>.
- Boulenger, G.A., 1884. “1883”. On a collection of frogs from Yurimaguas, Huallaga River, Northern Peru. *Proc. Zool. Soc. Lond.* 1883, 635–638.
- Brown, J. L., Caldwell, J.P., Twomey, E.M., Melo-Sampaio, P.R., Souza, M.B.D., 2011a. *Ranitomeya toraro*, in: A Taxonomic Revision of the Neotropical Poison Frog Genus *Ranitomeya* (Amphibia: Dendrobatidae). Magnolia Press, Auckland, New Zealand, pp. 42–47.
- Brown, J.L., Schulte, R., Summers, K., 2006. A new species of *Dendrobates* (Anura: Dendrobatidae) from the Amazonian lowlands in Peru. *Zootaxa* 1152, 45–58.
- Brown, J.L., Twomey, E.M., 2009. Complicated histories: three new species of poison frogs of the genus *Ameerega* (Anura: Dendrobatidae) from north-central Peru. *Zootaxa* 2049 (1), 1–38.
- Brown, J.L., Twomey, E., Amézquita, A., Souza, M.B.D., Caldwell, J.P., Lötters, S., von May, R., Melo-Sampaio, P.R., Mejía-Vargas, D., Perez-Peña, P., Pepper, M., Poelman, E.H., Sanchez-Rodriguez, M., Summers, K., 2011b. A taxonomic revision of the Neotropical poison frog genus *Ranitomeya* (Amphibia: Dendrobatidae). *Zootaxa* 3083, 1–120.
- Brown, J.L., Twomey, E., Pepper, M., Rodriguez, M.S., 2008. Revision of the *Ranitomeya fantastica* species complex with description of two new species from Central Peru (Anura: Dendrobatidae). *Zootaxa* 1823, 1–24. <https://doi.org/10.11646/zootaxa.1823.1.1>.
- Brown, J.L., Weber, J.J., Alvarado-Serrano, D.F., Hickerson, M.J., Franks, S.J., Carnaval, A.C., 2016. Predicting the genetic consequences of future climate change: The power of coupling spatial demography, the coalescent, and historical landscape changes. *Am. J. Bot.* 103, 153–163. <https://doi.org/10.3732/ajb.1500117>.
- Campbell, K.E., Frailey, C.D., Romero-Pittman, L., 2006. The Pan-Amazonian Ucayali Peneplain, late Neogene sedimentation in Amazonia, and the birth of the modern Amazon River system. *Palaeogeogr. Palaeoclimatol. Palaeoecol.* 239 (1–2), 166–219. <https://doi.org/10.1016/j.palaeo.2006.01.020>.
- Church, S.H., Ryan, J.F., Dunn, C.W., 2015. Automation and evaluation of the SOWH test with SOWHAT. *Syst. Biol.* 64 (6), 1048–1058.
- Clough, M., Summers, K., 2000. Phylogenetic systematics and biogeography of the poison frogs: evidence from mitochondrial DNA sequences. *Biol. J. Linn. Soc.* 70, 515–540. <https://doi.org/10.1111/j.1095-8312.2000.tb01236.x>.
- Darst, C.R., Cannatella, D.C., 2004. Novel relationships among hyloid frogs inferred from 12S and 16S mitochondrial DNA sequences. *Mol. Phylogenet. Evol.* 31 (2), 462–475. <https://doi.org/10.1016/j.ympev.2003.09.003>.
- Edgar, R.C., 2004. MUSCLE: multiple sequence alignment with high accuracy and high throughput. *Nucleic Acids Res.* 32 (5), 1792–1797. <https://doi.org/10.1093/nar/gkh340>.
- Faircloth, B.C., 2013. IllumiProcessor: A Trimmomatic wrapper for parallel adapter and quality trimming.
- Faircloth, B.C., 2016. PHYLUCE is a software package for the analysis of conserved genomic loci. *Bioinformatics* 32 (5), 786–788. <https://doi.org/10.1093/bioinformatics/btv646>.
- Faircloth, B.C., McCormack, J.E., Crawford, N.G., Harvey, M.G., Brumfield, R.T., Glenn, T.C., 2012. Ultraconserved Elements Anchor Thousands of Genetic Markers Spanning Multiple Evolutionary Timescales. *Syst. Biol.* 61, 717–726. <https://doi.org/10.1093/sysbio/sys004>.
- Goldman, N., Anderson, J.P., Rodrigo, A.G., 2000. Likelihood-based tests of topologies in phylogenetics. *Syst. Biol.* 49, 652–670.
- Grabherr, M.G., Haas, B.J., Yassour, M., Levin, J.Z., Thompson, D.A., Amit, I., Adiconis, X., Fan, L., Raychowdhury, R., Zeng, Q., Chen, Z., Mauceli, E., Hacohen, N., Gnirke, A., Rhind, N., di Palma, F., Birren, B.W., Nusbaum, C., Lindblad-Toh, K., Friedman, M., Regev, A., 2011. Full-length transcriptome assembly from RNA-Seq data without a reference genome. *Nat. Biotechnol.* 29 (7), 644–652. <https://doi.org/10.1038/nbt.1883>.
- Grant, T., Frost, D.R., Caldwell, J.P., Gagliardo, R., Haddad, C.F.B., Kok, P.J.R., Means, D.B., Noonan, B.P., Schargel, W.E., Wheeler, W.C., 2006. Phylogenetic systematics of dart-poison frogs and their relatives (Amphibia: Anura: Dendrobatidae). *Bull. Am. Mus. Nat. Hist.* 299, 1–262. [https://doi.org/10.1206/0003-0090\(2006\)299\[1:PSODFA\]2.0.CO;2](https://doi.org/10.1206/0003-0090(2006)299[1:PSODFA]2.0.CO;2).
- Grant, T., Rada, M., Anganoy-Criollo, M., Batista, A., Dias, P.H., Jeckel, A.M., Machado, D.J., Rueda-Almonacid, J.V., 2017. Phylogenetic Systematics of Dart-Poison Frogs and Their Relatives Revisited (Anura: Dendrobatoidea). *South Am. J. Herpetol.* 12 (s1), S1–S90. <https://doi.org/10.2994/SAJH-D-17-00017.110.2994/SAJH-D-17-00017.1.s9>.
- Guillory, W.X., French, C.M., Twomey, E.M., Chávez, G., Prates, I., von May, R., De la Riva, I., Lötters, S., Reichle, S., Serrano-Rojas, S.J., Whitworth, A., Brown, J.L., 2020. Phylogenetic relationships and systematics of the Amazonian poison frog genus *Ameerega* using ultraconserved genomic elements. *Mol. Phylogenet. Evol.* 142, 106638. <https://doi.org/10.1016/j.ympev.2019.106638>.
- Guillory, W.X., Muell, M.R., Summers, K., Brown, J.L., 2019. Phylogenomic Reconstruction of the Neotropical Poison Frogs (Dendrobatidae) and Their Conservation. *Diversity* 11, 126. <https://doi.org/10.3390/d11080126>.
- Heibl, C., 2008. PHYLOCH: R language tree plotting tools and interfaces to diverse phylogenetic software packages.
- Hoorn, C., Wesselingh, F.P., ter Steege, H., Bermudez, M., Mora, A., Sevink, J., Sanmartín, I., Sanchez-Meseguer, A., Anderson, C.L., Figueiredo, J.P., Jaramillo, C., Riff, D., Negri, F.R., Hooghiemstra, H., Lundberg, J., Stadler, T., Särkinen, T., Antonelli, A., 2010. Amazonia Through Time: Andean Uplift, Climate Change, Landscape Evolution, and Biodiversity. *Science* 330 (6006), 927–931.
- Hosner, P.A., Faircloth, B.C., Glenn, T.C., Braun, E.L., Kimball, R.T., 2016. Avoiding Missing Data Biases in Phylogenomic Inference: An Empirical Study in the Landfowl (Aves: Galliformes). *Mol. Biol. Evol.* 33 (4), 1110–1125. <https://doi.org/10.1093/molbev/msv347>.
- Kalyaanamoorthy, S., Minh, B.Q., Wong, T.K.F., von Haeseler, A., Jermin, L.S., 2017. ModelFinder: fast model selection for accurate phylogenetic estimates. *Nat. Methods* 14 (6), 587–589.
- Kapan, D.D., 2001. Three-butterfly system provides a field test of Müllerian mimicry. *Nature* 409 (6818), 338–340.
- Kozel, B., 2002. Three Men in a Raft: an Improbable Journey Down the Amazon, 1st ed. Pan Macmillan Australia, Sydney, Australia.
- Mallet, JAMES, Gilbert, L.E., 1995. Why are there so many mimicry rings? Correlations between habitat, behaviour and mimicry in *Heliconius* butterflies. *Biol. J. Linn. Soc.* 55 (2), 159–180.
- Minh, B.Q., Hahn, M.W., Lanfear, R., 2020. New methods to calculate concordance factors for phylogenomic datasets. *Mol. Biol. Evol.* 37, 2727–2733.
- Minh, B.Q., Nguyen, M.A.T., von Haeseler, A., 2013. Ultrafast Approximation for Phylogenetic Bootstrap. *Mol. Biol. Evol.* 30 (5), 1188–1195. <https://doi.org/10.1093/molbev/mst024>.
- Morales, V., 1992. Dos especies nuevas de *Dendrobates* (Anura: Dendrobatidae) para Perú. *Caribb. J. Sci.* 28, 191–199.
- Myers, C.W., 1982. Spotted poison frogs: description of three new *Dendrobates* from Western Amazonia, and resurrection of a lost species from “Chiriquí”. *Am. Mus. Novit.* 2721, 23.
- Nguyen, L.T., Schmidt, H.A., von Haeseler, A., Minh, B.Q., 2015. IQ-TREE: A Fast and Effective Stochastic Algorithm for Estimating Maximum-Likelihood Phylogenies. *Mol. Biol. Evol.* 32, 268–274. <https://doi.org/10.1093/molbev/msu300>.
- Noonan, B.P., Comeault, A.A., 2009. The role of predator selection on polymorphic aposematic poison frogs. *Biol. Lett.* 5 (1), 51–54.
- Noonan, B.P., Wray, K.P., 2006. Neotropical diversification: the effects of a complex history on diversity within the poison frog genus *Dendrobates*. *J. Biogeogr.* 33 (6), 1007–1020. <https://doi.org/10.1111/j.1365-2699.2006.01483.x>.
- Perez-Peña, P.E., Chavez, G., Twomey, E., Brown, J.L., 2010. Two new species of *Ranitomeya* (Anura: Dendrobatidae) from eastern Amazonian Peru. *Zootaxa* 2439 (1), 1–23.
- Persons, N.W., Hosner, P.A., Meiklejohn, K.A., Braun, E.L., Kimball, R.T., 2016. Sorting out relationships among the grouse and ptarmigan using intron, mitochondrial, and ultra-conserved element sequences. *Mol. Phylogenet. Evol.* 98, 123–132. <https://doi.org/10.1016/j.ympev.2016.02.003>.
- Prates, I., Paz, A., Brown, J.L., Carnaval, A.C., 2019. Links between prey assemblages and poison frog toxins: a landscape ecology approach to assess how biotic interactions affect species phenotypes. *Ecol. Evol.* 9 (24), 14317–14329.
- Prates, I., Xue, A.T., Brown, J.L., Alvarado-Serrano, D.F., Rodrigues, M.T., Hickerson, M.J., Carnaval, A.C., 2016. Inferring responses to climate dynamics from historical demography in neotropical forest lizards. *Proc. Natl. Acad. Sci.* 113 (29), 7978–7985.
- R Core Team, 2015. R: a language and environment for statistical computing.
- Pyron, R.A., Wiens, J.J., 2011. A large-scale phylogeny of Amphibia including over 2800 species, and a revised classification of extant frogs, salamanders, and caecilians. *Mol. Phylogenet. Evol.* 61 (2), 543–583. <https://doi.org/10.1016/j.ympev.2011.06.012>.
- Rambaut, A., Drummond, A.J., Xie, D., Baele, G., Suchard, M.A., 2018. Posterior Summarization in Bayesian Phylogenetics using Tracer 1.7. *Syst. Bio.* 67, 901–904.
- Ribas, C.C., Aleixo, A., Nogueira, A.C.R., Miyaki, C.Y., Cracraft, J., 2012. A palaeobiogeographic model for biotic diversification within Amazonia over the past three million years. *Proc. R. Soc. Lond.* 279 (1729), 681–689.
- Roberts, J.L., Brown, J.L., May, R.V., Arizabal, W., Schulte, R., Summers, K., 2006. Genetic divergence and speciation in lowland and montane Peruvian poison frogs. *Mol. Phylogenet. Evol.* 41 (1), 149–164. <https://doi.org/10.1016/j.ympev.2006.05.005>.
- de Fátima Rossetti, D., Mann de Toledo, P., Góes, A.M., 2005. New geological framework for Western Amazonia (Brazil) and implications for biogeography and evolution. *Quat. Res.* 63 (1), 78–89.
- Santos, J.C., Coloma, L.A., Cannatella, D.C., 2003. Multiple, recurring origins of aposematism and diet specialization in poison frogs. *Proc. Natl. Acad. Sci.* 100 (22), 12792–12797. <https://doi.org/10.1073/pnas.2133521100>.
- Santos, J.C., Coloma, L.A., Summers, K., Caldwell, J.P., Ree, R., Cannatella, D.C., Moritz, C., 2009. Amazonian Amphibian Diversity Is Primarily Derived from Late Miocene Andean Lineages. *PLoS Biol.* 7 (3), e1000056. <https://doi.org/10.1371/journal.pbio.1000056>.
- Schulte, R., 1986. Eine neue *Dendrobates*-Art aus Ostperu (Amphibia: Salientia: Dendrobatidae). *Sauria* 8, 11–20.
- Schulte, R., 1999. Pfeilgiftfrösche “Artenteil - Peru”. INBICO, Wailblingen, Germany.
- Sherratt, T.N., 2008. The evolution of Müllerian mimicry. *Naturwissenschaften* 95, 681.
- Shreve, B., 1935. On a new Teiid and Amphibia from Panama, Ecuador, and Paraguay. *Occas. Pap. Boston Soc. Nat. Hist.* 8, 209–218.
- Streicher, J.W., Wiens, J.J., 2017. Phylogenomic analyses of more than 4000 nuclear loci resolve the origin of snakes among lizard families. *Biol. Lett.* 13 (9), 20170393. <https://doi.org/10.1098/rsbl.2017.0393>.
- Stuckert, A.M.M., Venegas, P.J., Summers, K., 2014. Experimental evidence for predator learning and Müllerian mimicry in Peruvian poison frogs (*Ranitomeya*, Dendrobatidae). *Evol. Ecol.* 28 (3), 413–426.
- Summers, K., Bermingham, E., Weigt, L., McCafferty, S., Dahistrom, L., 1997. Phenotypic and Genetic Divergence in Three Species of Dart-Poison Frogs With Contrasting

- Parental Behavior. *J. Hered.* 88 (1), 8–13. <https://doi.org/10.1093/oxfordjournals.jhered.a023065>.
- Summers, K., Cronin, T.W., Kennedy, T., 2003. Variation in spectral reflectance among populations of *Dendrobates pumilio*, the strawberry poison frog, in the Bocas del Toro Archipelago. *Panama. J. Biogeogr.* 30, 35–53. <https://doi.org/10.1046/j.1365-2699.2003.00795.x>.
- Summers, K., Weigt, L.A., Boag, P., Bermingham, E., 1999. The Evolution of Female Parental Care in Poison Frogs of the Genus *Dendrobates*: Evidence from Mitochondrial DNA Sequences. *Herpetologica* 55, 254–270.
- Swofford, D.L., Olsen, G.J., Waddell, P.J., Hillis, D.M., 1996. Phylogenetic inference. In: Hillis, D.M., Moritz, C., Mable, B.K. (Eds.), *Molecular Systematics*, 2nd Edition. Sinauer Associates, Sunderland (MA), pp. 407–514.
- Symula, R., Schulte, R., Summers, K., 2001. Molecular phylogenetic evidence for a mimetic radiation in Peruvian poison frogs supports a Müllerian mimicry hypothesis. *Proc. R. Soc. Lond. B Biol. Sci.* 268 (1484), 2415–2421. <https://doi.org/10.1098/rspb.2001.1812>.
- Symula, R., Schulte, R., Summers, K., 2003. Molecular systematics and phylogeography of Amazonian poison frogs of the genus *Dendrobates*. *Mol. Phylogenet. Evol.* 26 (3), 452–475. [https://doi.org/10.1016/S1055-7903\(02\)00367-6](https://doi.org/10.1016/S1055-7903(02)00367-6).
- Twomey, E., Brown, J.L., 2008. Spotted poison frogs: rediscovery of a lost species and a new genus (Anura: Dendrobatidae) from northwestern Peru. *Herpetologica* 64 (1), 121–137. <https://doi.org/10.1655/07-009.1>.
- Twomey, E., Brown, J.L., 2009. Another new species of *Ranitomeya* (Anura: Dendrobatidae) from Amazonian Colombia. *Zootaxa* 2302, 48–60. <https://doi.org/10.11646/zootaxa.2302.1.4>.
- Twomey, E., Kain, M., Claeys, M., Summers, K., Castroviejo-Fisher, S., Van Bocklaer, I., 2020. Mechanisms for color convergence in a mimetic radiation of poison frogs. *Am. Nat.* 195 (5), E132–E149.
- Vences, M., Kosuch, J., Lötters, S., Widmer, A., Jungfer, K.-H., Köhler, J., Veith, M., 2000. Phylogeny and Classification of Poison Frogs (Amphibia: Dendrobatidae), Based on Mitochondrial 16S and 12S Ribosomal RNA Gene Sequences. *Mol. Phylogenet. Evol.* 15 (1), 34–40. <https://doi.org/10.1006/mpev.1999.0738>.
- Wollenberg, K.C., Veith, M., Noonan, B.P., Lötters, S., 2006. Polymorphism Versus Species Richness—systematics of Large *Dendrobates* from the Eastern Guiana Shield (Amphibia: Dendrobatidae). *Copeia* 2006, 623–629. [https://doi.org/10.1643/0045-8511\(2006\)6\[623:PVSROL\]2.0.CO;2](https://doi.org/10.1643/0045-8511(2006)6[623:PVSROL]2.0.CO;2).
- Yang, Z., 2007. PAML 4: Phylogenetic Analysis by Maximum Likelihood. *Mol. Biol. Evol.* 24, 1586–1591. <https://doi.org/10.1093/molbev/msm088>.
- Zerbino, D.R., Birney, E., 2008. Velvet: Algorithms for de novo short read assembly using de Bruijn graphs. *Genome Res.* 18 (5), 821–829. <https://doi.org/10.1101/gr.074492.107>.
- Zhang, C., Rabiee, M., Sayyari, E., Mirarab, S., 2018. ASTRAL-III: polynomial time species tree reconstruction from partially resolved gene trees. *BMC Bioinformatics* 19, 153. <https://doi.org/10.1186/s12859-018-2129-y>.
- Zimmermann, H., Zimmermann, E., 1988. Etho-Taxonomie und zoogeographische Artengruppenbildung bei Pfeilgiftfroschen (Anura: Dendrobatidae). *Salamandra* 24, 125–160.